

# The Frequency-Domain Multi-Distance Method in the Presence of Curved Boundaries

Albert Cerussi, John Maier, Sergio Fantini, Maria Angela Franceschini, and Enrico Gratton

Laboratory for Fluorescence Dynamics  
University of Illinois at Urbana-Champaign  
Department of Physics  
1110 West Green Street, Urbana, IL 61801-3080

## Abstract

We present experiments designed to test the applicability of the frequency-domain semi-infinite multi-distance method to cylindrical boundaries. Material with absorption and reduced scattering coefficients similar to those of tissue exposed to near-infrared light was cast into five cylindrical phantoms ranging in diameter from 4.2 to 10.2 cm, and also into a semi-infinite control. Measurements performed along the long axis of symmetry on the larger diameter cylinders reliably recovered both the absorption and the reduced scattering coefficients within 10% of the control values. Measurements performed along the circumference yielded values for these optical coefficients that differed significantly from the control values. These findings are explained by observing the measured frequency-domain parameters as functions of source-detector separation.

## Key Words

Light propagation in tissues, Multiple scattering, Spectroscopy - tissue diagnostics, Spectroscopic instrumentation

## I. Introduction

### A. Near-infrared Tissue Spectroscopy

The near-infrared (near-IR) part of the spectrum possesses many characteristics that are useful for the study of biological tissues [1]. Non-ionizing near-IR photons are absorbed weakly by water, which permits both low local heating and deep tissue penetration (several centimeters). Near-IR radiation is therefore a

favorable choice for a non-invasive diagnostic tool that has many clinical applications [2]. However, non-invasive optical methods are difficult in medicine since light transport in tissues is dominated by multiple scattering with mean-free-paths on the order of 30  $\mu\text{m}$  in tissues [3].

Diffusion theory offers a simple model that is used widely to describe multiple scattering processes. Over the last decade, diffusion theory has been successfully applied to tissue-like phantoms, allowing the extraction of absorption spectra from multiple scattering media [4-7]. Newly developed instruments that rely upon diffusion theory can measure the absorption properties of chromophores within highly scattering media [8, 9]. These instruments may be useful for both tissue spectroscopy and imaging. For example, the measurement of oxygen saturation (fraction of hemoglobin carrying oxygen) in human limbs may lead to the characterization of peripheral vascular disease (i.e., poor circulation) [2].

### B. The Difficulties of Boundaries

Boundary conditions severely limit diffusion theory. The very presence of any boundary violates one of the approximations of diffusion theory, namely that it is valid only at source-detector separations that are many scattering events removed from non-isotropic disturbances [10]. Finite boundaries, especially ones with curvature, are unavoidable in the real world of non-invasive tissue diagnostic monitoring. The infinite medium is hardly an adequate geometry for non-invasive applications. The semi-infinite geometry is more practical, but cylindrical and spherical geometries more closely resemble human limbs and heads. The frequency-domain multi-distance method with a single modulation frequency as presented by Fantini *et al.*

offers analytic solutions in both infinite [7] and semi-infinite [11] geometries. However, analytic solutions for curved geometries are difficult to obtain [12].

### C. Purpose of Study

Absolute values of measured frequency-domain parameters (*AC* intensity, *DC* intensity, and phase) change significantly between the infinite and the semi-infinite geometry. Yet some *relative changes* in these measured parameters are remarkably similar in both geometries. Keeping this in mind, *our goal was to apply the semi-infinite multi-distance method to curved boundaries*. This required checking that the relative changes in the data are unaffected by curvature.

This paper presents the results of our investigations of near-IR light transport inside cylindrical tissue-like phantoms. Using the semi-infinite multi-distance method, we measured the *absorption coefficient* ( $\mu_a$ ) and the *reduced scattering coefficient* ( $\mu_s'$ ) of a multiple scattering material cast into five cylinders of varying diameter and into a semi-infinite control sample. We then observed if this semi-infinite multi-distance method could mask perturbations to the semi-infinite boundary (i.e., curvature).

## II. Theory

The diffusion equation relates the scattering and absorption characteristics of a macroscopically homogeneous multiple scattering medium to the measurable photon density,  $U(r,t)$  (photons $\times$ cm $^{-3}$ ). In the frequency-domain approach, we modulate a point source of light at an angular frequency  $\omega$  (rad $\times$ s $^{-1}$ ). This creates a photon density of the form

$$U(r,\omega,t) = U_{DC}(r) + U_{AC}(r,\omega)e^{-i\omega t}, \quad (1)$$

where  $r$  (cm) denotes the separation between the source and the detector. Solutions to the diffusion equation in the infinite medium take the form of heavily damped spherical photon density waves [13]:

$$U_{AC}(r,\omega) = \frac{P(\omega)}{4\pi v D} \frac{1}{r} \exp[-k(\omega)r], \quad (2)$$

where  $ik(\omega) = i \left[ \frac{\mu_a}{D} \left( 1 - \frac{i\omega}{v\mu_a} \right) \right]^{\frac{1}{2}}$  is a complex wave-vector (cm $^{-1}$ ),  $v$  is the speed of the photons (cm $\times$ s $^{-1}$ ), assumed to be that of light in water,  $P(\omega)$  is the source strength (photons $\times$ s $^{-1}$ ), and  $vD = v(3\mu_s')^{-1}$  is the diffusion coefficient (cm $^2$  $\times$ s $^{-1}$ ). The absorption coefficient  $\mu_a$  (cm $^{-1}$ ) represents the inverse of the average distance

that photons travel before being absorbed. The reduced scattering coefficient  $\mu_s'$  represents the inverse of an essentially isotropic scattering scale which is typically an order of magnitude greater than the actual mean-free-path between scatterers. Measurable parameters of the photon density wave include its amplitude ( $|U_{AC}(r,\omega)|$ , or *AC*), temporal average intensity ( $U_{DC}(r)$ , or *DC*), and its phase with respect to the source (the argument of  $U_{AC}(r,\omega)$ , or  $\phi$ ).

The method of images allows us to extend this solution to the semi-infinite geometry [5]. This creates problems for diffusion theory, since the photon density cannot incorporate vastly non-isotropic photon densities. Forcing  $U(r,t)$  to vanish upon an *extrapolated boundary* is a well-known method used in neutron diffusion calculations [10]. Taking into account an index of refraction mismatch (i.e., internal reflections) between the tissue and the outside medium leads to an extrapolated boundary located about 0.1 cm above the semi-infinite boundary [14].

Semi-infinite expressions for each of the measurable frequency-domain parameters take the forms [11]:

$$\ln[U_{DC} F_{DC}(r, \mu_a, D)] = -r \left[ \frac{\mu_a}{D} \right]^{\frac{1}{2}} + G_{DC}(D, P(0)) \quad (3)$$

$$\ln[U_{AC} F_{AC}(r, \mu_a, D, \omega)] = -r \left[ \frac{\mu_a}{2D} \right]^{\frac{1}{2}} V_+(\mu_a, \omega) + G_{AC}(D, P(\omega)) \quad (4)$$

$$\phi = r \left[ \frac{\mu_a}{2D} \right]^{\frac{1}{2}} V_-(\mu_a, \omega) - \tan^{-1} [F_{PH}(r, \mu_a, D, \omega)] \quad (5)$$

where  $V_{\pm}(\mu_a, \omega) = \left[ \left[ 1 + \left( \frac{\omega}{v\mu_a} \right)^2 \right]^{\frac{1}{2}} \pm 1 \right]^{\frac{1}{2}}$ .

$F_{DC}$ ,  $F_{AC}$ ,  $F_{PH}$ ,  $G_{DC}$ , and  $G_{AC}$ , are known analytical functions of their arguments, and dependence upon boundary values such as the extrapolation distance have been omitted since they do not influence the following discussion.

Important points about these equations are:

- ① The left hand sides contain the *measurable* frequency-domain parameters ( $U_{DC}$ ,  $U_{AC}$ , and  $\phi$ ).
- ② Only the *intercepts* contain the information about the frequency-dependent source characteristics.
- ③ The only unknowns in the *slopes* of these lines are  $\mu_a$  and  $\mu_s'$ .

We can use the slopes associated with any two experimental quantities (such as  $AC$  and phase) to find the two unknowns  $\mu_a$  and  $\mu_s'$  using an iterative method. Since we modulate the source at a single frequency, the frequency-dependent intercepts need not be determined. In this work, slopes will always refer to the frequency-domain parameter measured versus  $r$ .

### III. Experiment

#### A. Samples

The tissue-like phantoms were made with hot-mold glue (scattering substance) and black India ink (absorbing substance). This material was cast into five cylinders with diameters between 4.2 cm and 10.2 cm, and also into a semi-infinite sample for a control. The optical coefficients of this material, measured on the control sample with the frequency-domain semi-infinite multi-distance method, were  $\mu_a = 0.0417 \pm 0.0007 \text{ cm}^{-1}$  and  $\mu_s' = 7.31 \pm 0.32 \text{ cm}^{-1}$ , which are typical for tissues exposed to near-IR light.

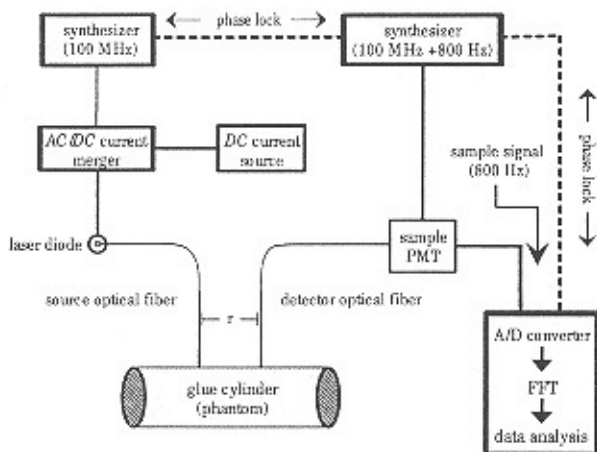


Fig. 1- Experimental setup. A 780 nm laser diode is intensity modulated by a sinusoidal 100 MHz current riding on a DC bias current. This light travels into the glue sample by a source optical fiber. The photon density wave is then sampled at a given  $r$  by moving the detector optical fiber. Collected light is then sent to a PMT, where after cross-correlation the signal is digitized, Fourier transformed, and then analyzed.

#### B. Instrument

The basic components of the frequency-domain instrument are presented in Fig. 1. A sinusoidal 100 MHz current signal riding on top of a DC bias current drives a 780 nm laser diode. The laser delivers its light to the sample with the help of a source fiber optic cable. A detector optical fiber placed at a distance  $r$  away from the source fiber on the surface of the phantom samples the photon density wave at that

location. We could move the location of the source fiber while keeping the detector fiber fixed because of machined templates that fit onto the sample. A photomultiplier tube (PMT) modulated at 100 MHz plus an 800 Hz offset, allows cross-correlation of the incoming signal. In other words, by beating the detector and incoming signal, we are able to translate a high-frequency (100 MHz) signal into a low-frequency (800 Hz) signal, while retaining phase and modulation information. The resulting 800 Hz signal is then digitized, Fourier transformed, and analyzed with a personal computer [15]. All components in the system are phase locked.

#### C. Protocol

We measured photon density waves over a range of  $r$ 's in a reflectance-style measurement. Several areas of the glue were measured to verify that it was homogeneous. There are also two possible directions along the surface that we could measure (Fig. 2):

- ① along the long axis of symmetry (i.e.,  $z$  axis)
- ② along the circumference.

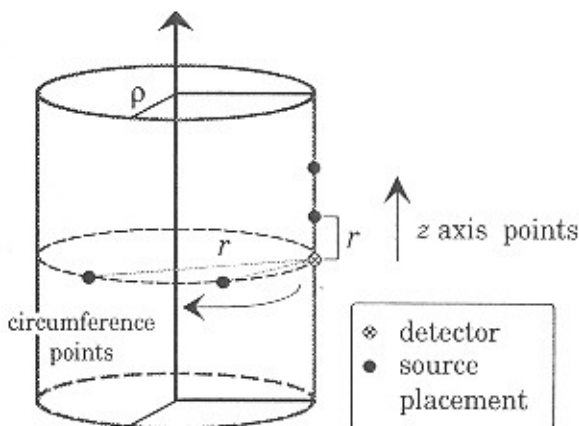


Fig. 2 - Diagram of the experimental geometry. The circle with the  $x$  inside represents the fixed detector location, and the blackened circles represent the individual placement locations of the source for each  $r$  in both  $z$  axis and circumference measurements. Note that  $r$  always refers to the straight-line separation between the source and the detector.

In both style measurements,  $r$  represents the *straight-line distance* between source and detector. The measurement was easily reproducible because of the use of machined templates that fit over the phantoms. Thus, the fiber placements were identical for a given measurement of each phantom. For the circumference style measurement, templates were available for only three of the cylinders.

## IV. Results

### A. Measured Frequency-Domain Parameters

First, we need to inspect the character of the measured data and decide if the semi-infinite multi-distance method is appropriate for cylinders. Figure 3 presents the measured relative phase shifts of the photon density wave for each of the three types of measurements. The squares are the phases measured on the control sample. Measurements performed on the cylinder (10.2 cm shown here) are presented using hour-glasses and triangles for the  $z$  axis and the circumference measurements, respectively. The solid lines are the best linear fit of the data. These are offset by an arbitrary amount to facilitate the comparison of the slopes.

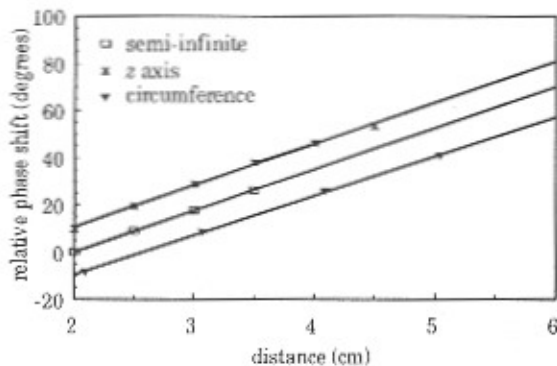


Fig. 3 - Comparison of phase slopes (vs.  $r$ ). The slopes of the phase measured along the  $z$  axis or along the circumference agree within 1% and 5% (respectively) of the control value. This indicates that the phase as a function of distance is not strongly influenced by the curvature for measurements performed on the cylinder.

Diffusion theory predicts an essentially linear phase vs.  $r$  (Eq. (5)). However, the phases are also essentially linear for both types of cylindrical measurements. The value of the phase slope measured along the  $z$  axis and the circumference agrees with the control value within 1% and 5%, respectively. The slopes of the phases have not been significantly affected by the curvature. On this cylinder, the largest  $r$  measured is about 5 cm, which corresponds to a polar angle of  $72^\circ$ .

Figure 4 presents the AC intensity using the same criteria as the previous plot, but all measurements were normalized. As before, the lines have been given an arbitrary offset to facilitate the comparison of the slopes. The  $AC^*$  represents the left hand side of Eq. (4). Here, the slopes of the control value and the slopes measured along the  $z$  axis on the cylinder agree within 1%. But the slopes measured along the circumference deviates by more than 40% from the control value. The AC slope for the circumference measurement lies somewhere between the infinite medium and semi-infinite medium value.

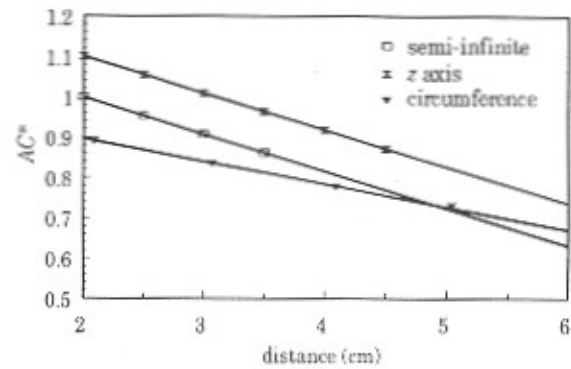


Fig. 4 - Comparison of AC slopes (vs.  $r$ ).  $AC^*$  refers to the left hand side of Eq. (4). The AC intensity measured along the  $z$  axis matches within 1% of the control value. However, the AC intensity measured along the circumference agrees very poorly with the control value.

### B. Measured Optical Coefficients

We found that the semi-infinite method was able to recover  $\mu_a$  within 9% and  $\mu_s'$  within 5% for all but the smallest diameter cylinder (4.2 cm) when the measurement was performed along the  $z$  axis. For reasons of signal to noise, we elected to use the AC & phase as our frequency-domain parameters. Figure 5(A) presents the  $\mu_a$  measured in the control and measured in the cylinders along the  $z$  axis. The dashed horizontal line represents the value measured in the semi-infinite control. The measured absorption coefficients lie within the experimental uncertainties for the larger cylinders. The reduced scattering is present in Fig. 5(B) in similar fashion. The variation in  $\mu_s'$  between cylinders in this measurement is small, but still the smallest cylinder has the poorest agreement with the control.

The absorption (Fig. 6(A)) and reduced scattering (Fig. 6(B)) measured along the circumference of the cylinders is a different story. This time, the effect of the curvature was much stronger, making the determination of  $\mu_a$  and  $\mu_s'$  quite difficult. The values determined along the circumference are approximately a factor of 2 below the semi-infinite control values.

## V. Discussion

Figure 3 demonstrates the linearity of the phase. Since the multi-distance method is based upon diffusion theory, the phase must be linear. Further, the curvature has changed the slope of the phase by only a few percent. This appears reasonable, when one considers that inhomogeneities placed inside of similar media affect the phase by only a degree or two.

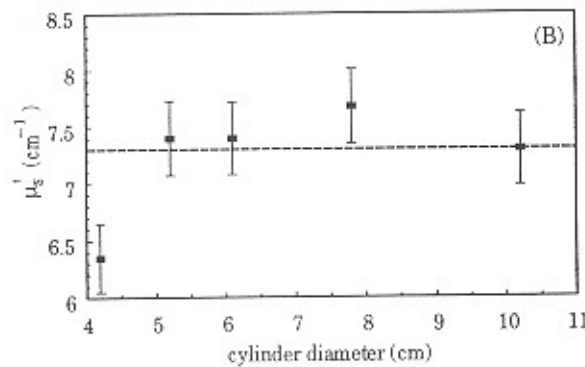
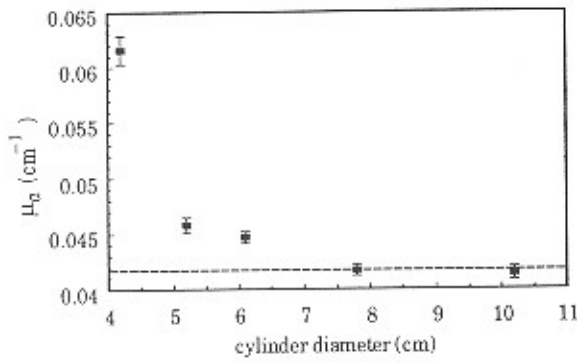


Fig. 5 - Optical coefficients of phantoms measured along the  $z$  axis. Plot (A) presents the absorption, and plot (B) presents the reduced scattering measured in the cylinders. The dashed solid line represents the control value determined from the semi-infinite sample in both plots. Note the apparent increase in measured  $\mu_a$  as the cylinder diameter decreases. Agreement with the control value lies within 9% for  $\mu_a$  and within 5% for  $\mu_s'$  for all cylinders, save the smallest one.

The  $z$  axis and circumference measurements differ in one major aspect. Each  $r$  sampled along the  $z$  axis is affected by the curvature in a similar fashion because of the symmetry about this axis. In the circumference measurement, each  $r$  will be affected very differently by the curvature. The larger  $r$ 's will be affected by curvature much less than the smaller  $r$ 's. Large  $r$ 's along the circumference will eventually wind up as transmission measurements (i.e.,  $180^\circ$  polar angle) rather than reflection measurements.

Failure to accurately determine the AC intensity slope for the circumference measurement explains why the circumference measurement failed to give the correct values of the optical coefficients. In the  $z$  axis measurement, both the AC slope and the phase slope agree very well with the control. We therefore expect to be able to accurately recover the optical coefficients if measured along the  $z$  axis. This is indeed the case, except for the small diameter cylinders (less than 5 cm in this study).

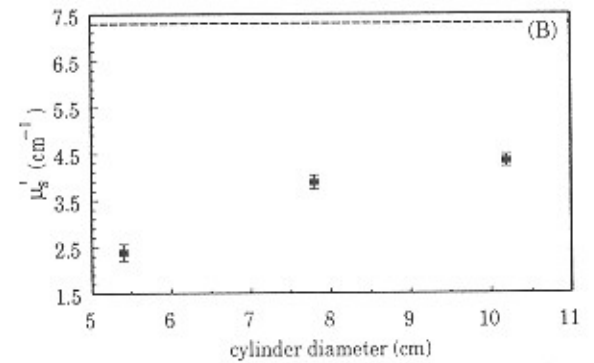
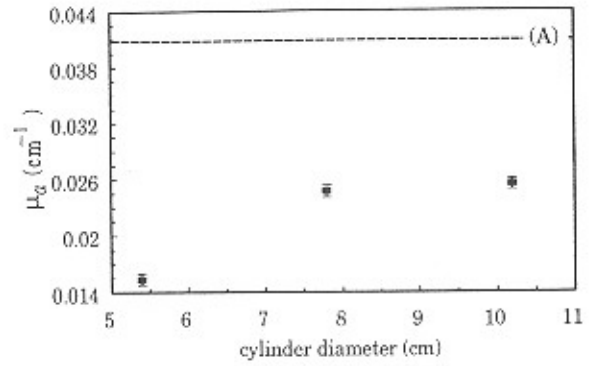


Fig. 6 - Optical coefficients of phantoms measured along the circumference. Plot (A) presents the absorption, and plot (B) presents the reduced scattering of the cylinders. The dashed solid line is the same as in Fig. 5. The optical coefficients are not close at all to the control values.

The success of the cylindrical measurements emerges from the fact that the multi-distance method turns slopes, and not absolute values, into absolute measurements of  $\mu_a$  and  $\mu_s'$ . Although the absolute values of directly measured quantities will be affected dramatically by the curved boundary, the relative changes with respect to  $r$  remain approximately the same. This is encouraging for current hemoglobin oxygenation measurements that are performed upon arms and legs [16]. Results obtained should not be affected significantly by curvature, provided that they are performed along the  $z$  axis.

Since the relative phase slope information is preserved in the cylindrical measurements, perhaps the best way to approach the problem of cylindrical boundaries is to use exclusively phase slope information. The slope of the phase is also dependent upon modulation frequency (Eq. (5)). Therefore, determining the phase slope at two modulation frequencies may provide a way to mask the effects of curvature for measurements performed along the

circumference. This gives hope for measurements that must be performed on the head.

## VI. Conclusion

The application of the frequency-domain semi-infinite multi-distance method along the axis of symmetry allowed us to accurately recover the absorption and reduced scattering coefficients of tissue-like cylindrical phantoms with diameters comparable to adult human limbs. This suggests that this method is valid despite the boundary effects of human limbs encountered by portable tissue spectrometers. The phase slope was not significantly affected by the curvature, and hence provides a useful parameter that is relatively insensitive to the boundary.

## VII. Acknowledgments

This work was performed at the Laboratory for Fluorescence Dynamics in Urbana, IL, and was supported by the National Institute of Health (grants RR03155 and CA57032) and the University of Illinois.

## VIII. References

- [1] D. A. Benaron and D. K. Stevenson, "Optical time-of-flight and absorbance imaging of biologic media," *Science* **259**, 1463-1466 (1993).
- [2] J. S. Maier, B. Barbieri, A. Chervu, I. Chervu, S. Fantini, M. A. Franceschini, M. Levi, W. M. Mantulin, A. Rosenberg, S. A. Walker, and E. Gratton, "In-Vivo study of human tissues with a portable near-infrared tissue spectrometer," *SPIE Proc.* **2387**, 240-248 (1995).
- [3] B. C. Wilson, M. S. Patterson, S. T. Flock, and D. R. Wyman, "Tissue optical properties in relation to light propagation models and *in-vivo* dosimetry," *Photon Migration in Tissues*, ed. by B. Chance, 25-42, (Plenum, New York, 1989).
- [4] J. B. Fishkin, P. T. C. So, A. E. Cerussi, S. Fantini, M. A. Franceschini, and E. Gratton, "Frequency-domain method for measuring spectral properties in multiple-scattering media: methemoglobin absorption spectrum in a tissuelike phantom," *Appl. Opt.* **34**, 1143-1155 (1995).
- [5] M. S. Patterson, B. Chance, and B. C. Wilson, "Time resolved reflectance and transmittance for the non-invasive measurement of tissue optical properties," *Appl. Opt.* **28**, 2331-2336 (1989).
- [6] E. M. Sevick, B. Chance, J. Leigh, S. Nioka, and M. Maris, "Quantitation of time- and frequency-resolved optical spectra for the determination of tissue oxygenation," *Anal. Biochem.* **195**, 330-351 (1991).
- [7] S. Fantini, M. A. Franceschini, J. B. Fishkin, B. Barbieri, and E. Gratton, "Quantitative determination of the absorption spectra of chromophores in strongly scattering media: a light emitting diode based technique," *Appl. Opt.* **33**, 5204-5213 (1994).
- [8] S. Fantini, M. A. Franceschini, J. S. Maier, S. A. Walker, B. Barbieri, and E. Gratton, "Frequency-domain multichannel optical detector for non-invasive tissue spectroscopy and oximetry," *Opt. Eng.* **34**, 32-42 (1995).
- [9] S. J. Madsen, E. R. Anderson, R. C. Haskell, and B. J. Tromberg, "Portable, high-bandwidth frequency-domain photon migration instrument for tissue spectroscopy," *Opt. Lett.* **19**, 1934-1936 (1994).
- [10] J. J. Duderstadt and L. J. Hamilton, *Nuclear Reactor Analysis* (John Wiley & Sons, New York, 1976).
- [11] S. Fantini, M. A. Franceschini, and E. Gratton, "Semi-infinite-geometry boundary problem for light migration in highly scattering media: a frequency-domain study in the diffusion approximation," *J. Opt. Soc. Am. B* **11**, 2128-2138 (1994).
- [12] S. R. Arridge, M. Cope, and D. T. Delpy, "The Theoretical basis for the determination of optical path lengths in tissue: temporal and frequency analysis," *Phys. Med. Biol.* **37**, 1531-1560 (1992).
- [13] J. B. Fishkin and E. Gratton "Propagation of photon-density waves in strongly scattering media containing an absorbing semi-infinite plane bounded by a straight edge," *J. Opt. Soc. Am. A.* **10**, 127-140 (1993).
- [14] M. Keijzer, W. M. Star, and P. M. Storchi, "Optical diffusion in layered media," *Appl. Opt.* **27**, 1820-1824 (1988).
- [15] B. Feddersen, D. W. Piston, and E. Gratton, "Digital parallel acquisition in frequency-domain fluorimetry," *Rev. Sci. Instr.* **60**, 2929-2936 (1989).
- [16] D. A. De Blasi, S. Fantini, M. A. Franceschini, and E. Gratton, "Cerebral and muscle oxygen saturation measurement by frequency-domain near infra-red spectrometer," *Med. & Biol. Eng. Comp.* **33**, 228-230 (1995).